Global optimization of quasi-monoenergetic electron beams from laser wakefield accelerators

Hai-En Tsai, Chih-Hao Pai, and M. C. Downer

Citation: AIP Conference Proceedings **1507**, 330 (2012); doi: 10.1063/1.4773717

View online: http://dx.doi.org/10.1063/1.4773717

View Table of Contents: http://scitation.aip.org/content/aip/proceeding/aipcp/1507?ver=pdfcov

Published by the AIP Publishing

Global Optimization of Quasi-Monoenergetic Electron Beams from Laser Wakefield Accelerators

Hai-En Tsai, Chih-Hao Pai and M. C. Downer

Department of Physics, The University of Texas at Austin, 1 University Station C1600, Austin, TX 78712-0284

Abstract. We globally optimize a terawatt-laser-driven wakefield accelerator by systematically varying laser and target parameters to achieve 100 MeV electrons, 10% energy spread, 100 pC charge, 4 mrad divergence and 10 mrad pointing fluctuation with ~100% reproducibility, thereby meeting conditions for producing ~10^6 200 keV X-ray photons/pulse by inverse Compton scatter**.**

Keywords: Laser-driven acceleration; Beam Characteristics; Hard X-ray Sources.
PACS: 41.75.Jv; 29.27.Fh; 52.59.Px

INTRODUCTION

Production of bright, coherent, femtosecond hard x-ray pulses by Compton backscatter from compact terawatt-laser-driven wakefield accelerator (LWFA) beams can open a range of ultrafast x-ray science to university laboratories [1], but because of low conversion efficiency and the instability of acceleration in the bubble regime [2] require careful optimization of charge, energy, energy spread, collimation and repeatability of the electron beam [3]. Here we report the global optimization of a LWFA by systematically varying laser and target parameters to achieve 100 MeV electrons, 10% energy spread, 100 pC charge, 4 mrad divergence and 10 mrad pointing fluctuation with ~100% reproducibility, thereby meeting conditions for producing ~10^6 200 keV X-ray photons/pulse by inverse Compton scatter.

EXPERIMENT

For experiments, 45 TW, 35 fs, 0.8 J, 810nm laser pulses (Fig. 1b) from the University of Texas Tri-color Terawatt Ti:sapphire system (UT^3) were focused with a f/12 parabolic mirror onto a 1-mm or 3-mm-long supersonic helium gas jet (SmartShell Co., Ltd.) hydrodynamically designed for "top-hat" density profile with 200 μm sharp edge (Fig. 2b). The incident beam was carefully optimized to achieve Strehl ratio >0.5, with focal spot 11 μm FWHM (Fig. 2a) and $I_0 = 5 \times 10^{18}$ W/cm^2 ($a_0 = 1.5$). Electron beam profiles were detected using a LANEX phosphor screen 30 cm downstream from the gas jet. Electron spectra were measured by inserting 1T permanent magnet between the jet and screen (Fig. 1a).

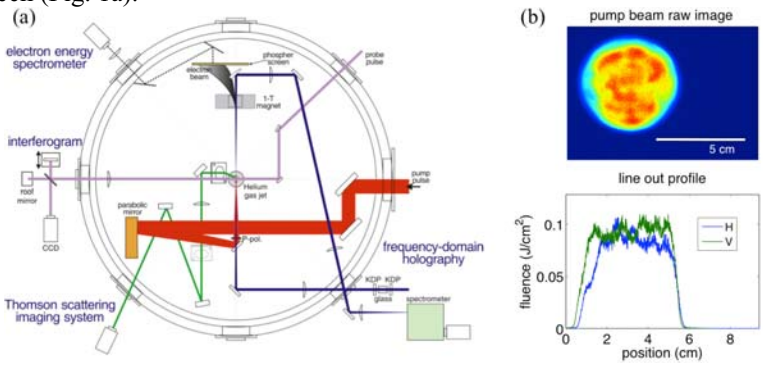

FIGURE 1. (a) Experimental layout. (b) 810 nm pump beam image and lineout profile.

Advanced Accelerator Concepts
AIP Conf. Proc. 1507, 330-335 (2012); doi: 10.1063/1.4773717

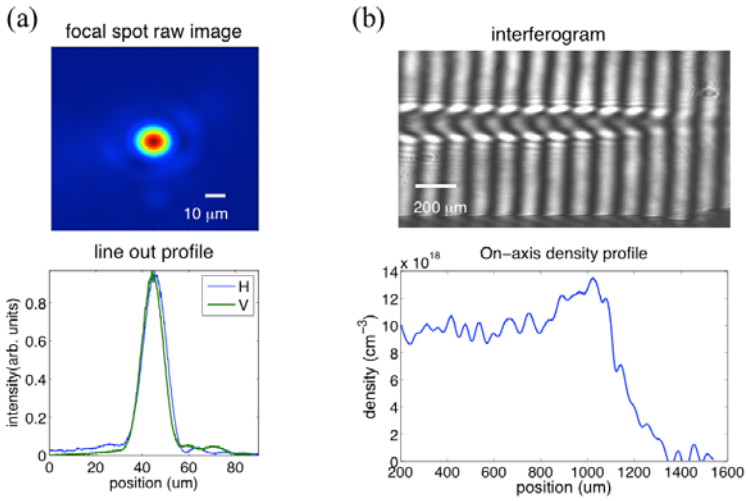

FIGURE 2. (a) Focal spot image and lineout profile. (b) Transverse interferogram taken at gas jet entrance of 1.6-mm field of view and on-axis density lineout profile

RESULTS

Here we demonstrate the generation of high-quality electron beams from a terawatt LWFA with 100% shot-to-shot reproducibility, average divergence 4 mrad (FWHM), 10 mrad r.m.s. pointing fluctuation, and average charge 100 pC at 100 MeV. The particular electron beam profile presented in Fig. 3a has only 2 mrad divergence (FWHM). The electron spectrum in Fig. 2b has a peak at 100 MeV and 10% energy spread. Both are obtained at an optimum acceleration condition, as discussed below, from a 3-mm He gas jet with 1.8 x 10^{19} cm^{-3} plasma density and 35 fs drive pulse duration.

In contrast, beams generated from a 1-mm He jet have average peak at 31 MeV with only 60% reproducibility, 19 mrad divergence, at an optimum plasma density of 2.2x10^{19} cm^{-3}.

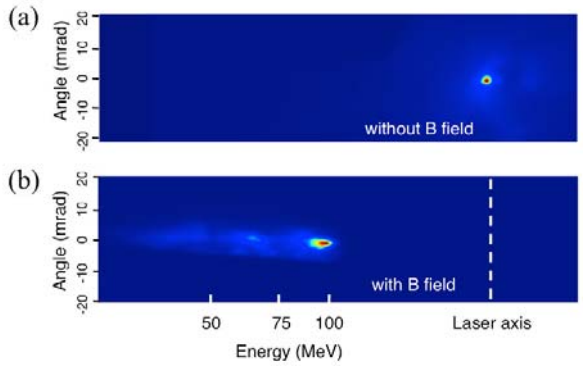

FIGURE 3. Raw images obtained on the LANEX screen. (a) Image of electron beam spatial distribution obtained from the LANEX screen when no magnetic field is applied. (b) Image obtained when magnetic field is applied showing that the electron beam is deviated from laser axis (the white vertical dashed line) and its position corresponds to 100 MeV. (a) and (b) are obtained at an optimum acceleration condition with a plasma density (n_e = 1.8 x 10^{19} cm^{-3}) and a pulse duration of 35 fs (FWHM).

Optimum Plasma Density

In order to achieve the optimum acceleration, we systematically and extensively investigated how charge, brightness, divergence, pointing, repeatability and energy spectra vary as functions of plasma density, pulse duration and focus position. We varied the plasma density at constant pulse energy (0.8 J on target), pulse duration, and focus position. First of all, the stable and optimum electron beam brightness and divergence were achieved in a narrow

range of plasma density (1.5 - 2 x 10^{19} cm^{-3}) for the shortest pulse duration (35 fs) showing in Fig. 4. The plasma density was linearly tuned by adjusting gas jet pressure. The averaged on-axis plasma density n_e was measured with a transverse interferometer.

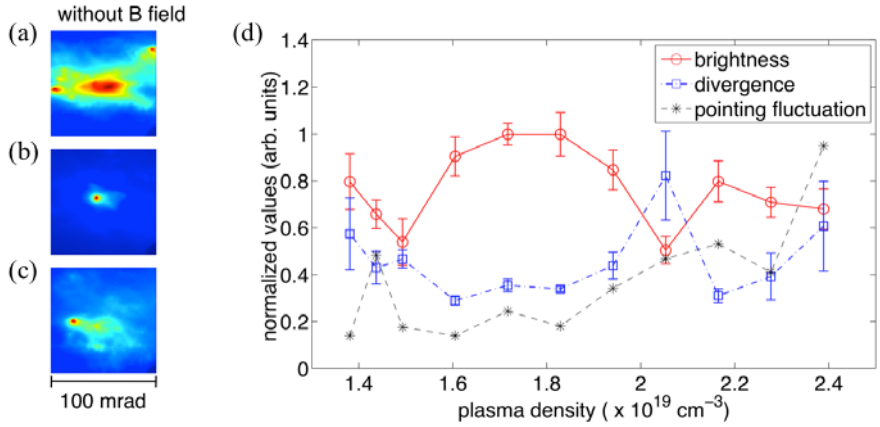

FIGURE 4. (a) - (c) Image obtained on LANEX without applying magnetic field at plasma density of 1.4, 1.8, and 2.4 x 10^{19} cm^{-3}. (d) The normalized brightness, divergence and pointing fluctuation vary as a function of plasma density (pulse duration fixed at 35 fs), where the brightness is evaluated by the peak intensity of the electron profile, the divergence is evaluated by the FWHM of a Gaussian curve fitted to the electron profile, the pointing fluctuation is derived from the standard deviation of the center position of the electron profile imaged on the LANEX screen. Every data point is obtained by averaging over 10-30 shots. Error bars indicate one standard deviation of the 10-30 shots.

In addition, when the electron density was increased from 1.8 x 10^{19} cm^{-3} to 2.4 x 10^{19} cm^{-3}, the electron spatial profiles split into several lobes (Fig. 4c) and the peak electron energy and number decreased (Fig. 5e). Below 1.5 x 10^{19} cm^{-3}, the divergence and pointing fluctuation of accelerated electrons increased dramatically (Fig. 4), although the distribution was still quasi mono-energetic (Fig. 5a).

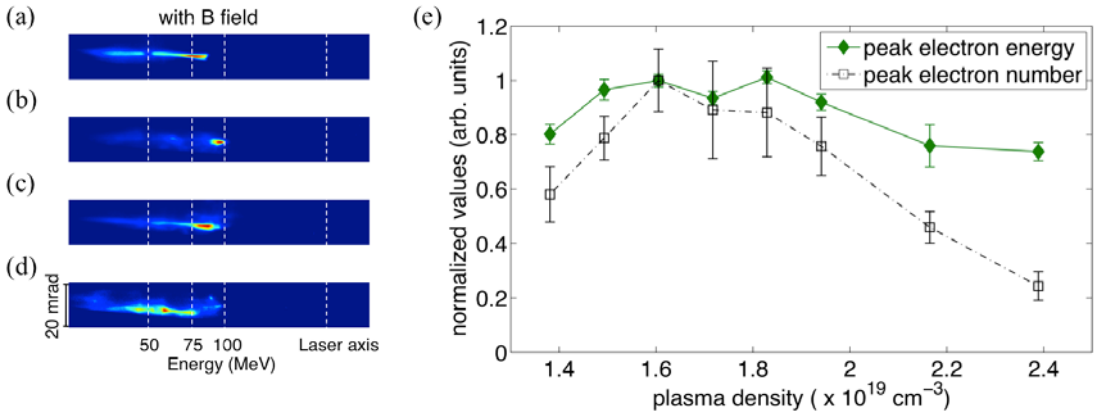

FIGURE 5. (a)-(d) Electron image obtained when magnetic field is applied at plasma density of 1.4, 1.8, 1.9 and 2.2 x 10^{19} cm^{-3}. (e) The normalized peak electron energy and peak electron number vary as a function of plasma density (pulse duration fixed at 35 fs). Peak electron energy is obtained from the peak position of the electron energy distribution as recorded on the LANEX screen with magnetic field applied; peak electron number is obtained by summing up all the electron number along spatial (vertical) axis at peak within a spectral width of 0.3 MeV, which is determined by spectrometer dispersion on a CCD pixel width (~0.3 MeV/pixel). Every data point is obtained by averaging over 10-30 shots. Error bars indicate one standard deviation of the 10-30 shots.

Optimum Pulse Duration

The pulse duration was varied at constant pulse energy by tuning separation of compressor gratings and was measured inside the vacuum chamber by a single-shot auto-correlator located near the target to avoid dispersion

from air and optics. We also conducted the experiment at various plasma densities higher and lower than 1.8 x 10^{19} cm^{-3} (optimum density). All the results showed the same trend that stable, optimum electron brightness, divergence, charge and peak energy were achieved with pulse duration shorter than 45 fs (Figs. 6 and 7). Increasing the pulse duration above 45 fs was sufficient to lose repeatability, small divergence and the stable peaked energy distribution. Simulations of previous work [4] also show that the quality of the electron beam is higher when trapped electrons do not interact with laser fields, which increases divergence and energy spread. The argument could explain why higher quality beams are obtained experimentally for shorter pulses and a narrow range of electron density.

The evolution of electron brightness, divergence, pointing, and spectra with our experimental parameters also indicates that pulses comparable or shorter than a plasma period are essential for high quality, mono-energetic electron acceleration.

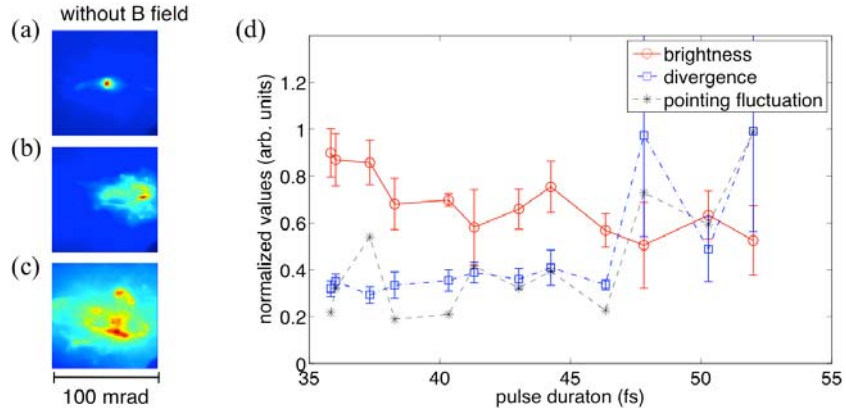

FIGURE 6. (a)-(c) Image obtained on LANEX without applying magnetic field at pulse duration of 35, 41, and 50 fs. (d) The normalized brightness, divergence and pointing fluctuation vary as a function of pulse duration (plasma density fixed at 1.8x10^{19} cm^{-3}. Brightness, divergence and pointing fluctuations are evaluated as described in the caption of Fig. 4.

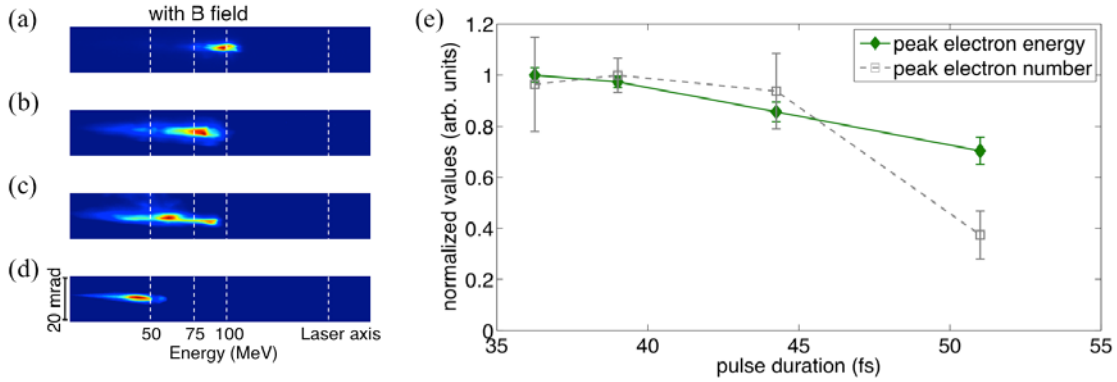

FIGURE 7. (a)-(d) Electron image obtained when magnetic field is applied at pulse duration of 36, 39, 44, and 51 fs. (e) The normalized peak electron energy and peak electron number vary as a function of pulse duration (plasma density fixed at 1.8x10^{19} cm^{-3}). Peak electron energy and peak electron number are evaluated as described in the caption of Fig. 5.

Optimum Focus Position

We also studied the influence of focus position of the laser pulse with respect to gas jet. Specifically, how the electron brightness, divergence and pointing fluctuation vary as functions of focus position along the laser propagation direction. The result in Figure 8 shows that the optimum acceleration happens when the focus is placed close to the front edge of gas jet (0-μm position in Fig. 8). The front edge of gas jet is defined as the center of 200-μm up ramp (Fig. 2b). The regime of stable acceleration is found to place the focus within ±250 μm. When the focus is moved away from the range of ±250 μm, the beam loses its pointing stability, small divergence and reproducibility.

Technically, we can examine the overlap of the focus position and gas jet edge from the transverse interferogram, which has a spatial resolution < 10 μm. Although the Rayleigh range of laser focus is ~850 μm, the focus center can still be located by lowering the laser intensity such that the ionization channel in interferogram is shorter than 100 μm. The optimum plasma density and pulse duration were all found when focus position was placed at the edge of gas jet.

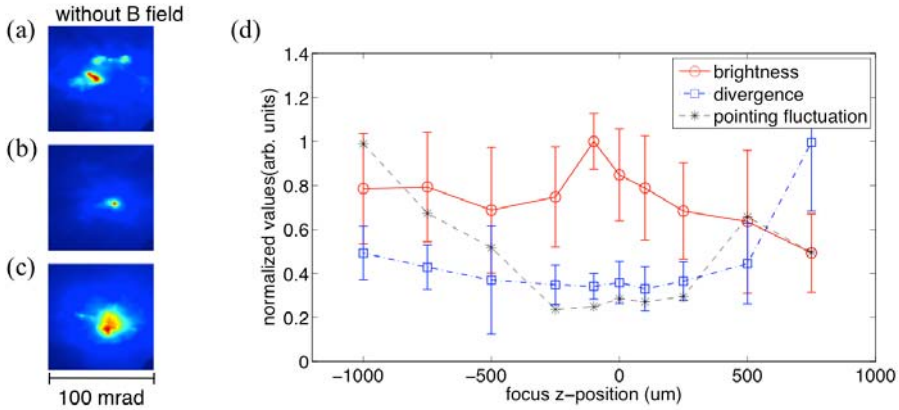

FIGURE 8. (a) - (c) Image obtained on LANEX without applying magnetic field placing focus position at -750 μm, +100 μm, +750 μm with respect to the front edge of gas jet. (d) The normalized brightness, divergence and pointing fluctuation vary as a function of focus position (pulse duration at 35 fs, plasma density at 1.8 x10^{19} cm^{-3}), where brightness, divergence and pointing fluctuations are evaluated as described in the caption of Fig. 4.

FUTURE WORK

The principal motivation behind careful optimization of a terawatt LWFA is to optimize the efficiency of coherent X-ray production via inverse Compton scattering. In our planned inverse Compton scattering experiment, the X-ray will be produced by the head on collision of a femtosecond laser pulse (30 mJ, 50 fs) split from pump pulse with the optimized LWFA 100 MeV (γ = 196) mono-energetic electron beam.

Calculations based on Esarey et al [2] show that the X-ray photon energy will peak at 230 keV given by

$$E_{x-ray} = \frac{4\gamma^2 E_{laser}}{1+(\gamma\theta)^2 + 4\gamma E_{laser}/(m_e c^2)} \approx 4\gamma^2 E_{laser} = 230KeV, \quad (1)$$

where E_{laser} is laser photon energy. The beam divergence angle is

$$\theta_{x-ray} \approx 1/\gamma = 5.1mrad, \quad (2)$$

The photon number/ photon energy can be calculated from the measured electron spectrum by

$$\frac{dN_x}{dE_x} = \frac{\alpha_f}{8E_{laser}} a_0^2 \gamma m_e c^2 N_0 \frac{dN_e}{dE_e} d\Omega, \quad (3)$$

where α_f is the fine-structure constant, a_0 is the laser vector potential, N_0 is the number of laser cycle, $d\Omega$ is collecting angle, dN_e/dE_e is electron number per electron energy. Therefore, X-ray spectrum based on the de-convoluted electron spectrum corresponding to Fig. 3b can be calculated. Integration over X-ray energy shows that 5 x 10^6 total hard X-ray photons/pulse can be generated.

We also compare our parameters and calculated X-ray photons with those from previous experiment [5] and simulation [1]. Table 1 shows the comparison result, in which our calculated photon numbers based on Eq. 3. match the photon numbers presented in previous work (* and **) within an order of magnitude. The calculated photon number/ shot in our case is 5 x 10^6, we can therefore estimate 10^6 - 10^7 photon number to be measured.

TABLE 1 The comparison of experimental parameters and inverse Compton scattered photon numbers between our case and other groups

	Our case	**Miura et al. PIF 2010**	**Hartemann et al. 2007**
γ	200	100	332
charge	$6.3\text{x}10^8$ (100pC)	$1.8\text{x}10^8$ (30pC)	$3\text{x}10^9$ (500pC)
N_0 (laser cycle)	14 (35 fs)	37 (100fs)	7.7 (21fs)
a_0	0.38	0.6	0.19
$\theta_{x\text{-}ray}$	5 mrad	5 mrad	10 mrad
X-ray photon number/shot from our calculation	$5\text{x}10^6$	$3.5\text{x}10^5$	$1.4\text{x}10^7$
X-ray photon number/shot		$1\text{x}10^5$ *	$2.95\text{x}10^7$ **

* Experiment result from [5]; ** Simulation result from [1]

ACKNOWLEDGMENTS

This work was supported by U.S. DOE grant DE-FG03-96ER40954 and NSF grant PHY-0936283.

REFERENCES

1. F. V. Hartemann *et al*., "Compton scattering x-ray sources driven by laser wakefield acceleration", *Phys. Rev. ST-AB* **10**, 011301 (2007).
2. A. Pukhov and J. Meyer-ter-Vehn, "Laser wake field acceleration: the highly non-linear broken-wave regime", *Appl. Phys. B* **74**, 355–361 (2002).
3. E. Esarey *et al*. "Nonlinear Thomson scattering of intense laser pulses from beams and plasmas", *Phys. Rev. E* **48**, 3003 (1993).
4. J. Faure *et al*. "A laser-plasma accelerator producing monoenergetic electron beams", *Nature* **431,** 737 (2004).
5. E. Miura *et al*. "X-ray generation via laser compton scattering by laser-accelerated electron beam", *Physics in Intense Fields* (2010).